SEED LOCALIZATION USING TRUS AND GRF BASED GAUSSIAN FILTERING FOR BRACHYTHERAPY APPLICATIONS

Varsha Sampath [1], Vladimir Misic [2], Eli Saber [1], Haisong Liu [2], Yan Yu [2]

1. Electrical Engineering Department, Rochester Institute of Technology, Rochester NY
2. Radiation Oncology, University of Rochester Medical Center, Rochester NY

ABSTRACT

In this paper, we propose a novel algorithm for detecting needles and their corresponding implanted radioactive seed locations in the prostate during Brachytherapy from trans-rectal ultrasound images. This is carried out efficiently using separable Gaussian filters in a probabilistic Gibbs random field framework. An approximation of the needle path through the prostate volume is obtained using a polynomial fit. The seeds are then detected and assigned to their corresponding needles by calculating local maxima. In our experiments, we were able to successfully localize over 85% of the implanted seeds.

Keywords: Brachytherapy, Gibbs Random Fields.

1. INTRODUCTION

Prostate cancer is one of the most commonly diagnosed non-skin cancers in men. Typical treatment procedures include radical prostectomy, external beam radiotherapy, and brachytherapy, dependent on the stage of the detected cancer and the patient's preference. Brachytherapy is a minimally invasive method that uses hollow needles to implant radioactive seeds for treating cancerous cells. It relies on real-time visualization (thus, often called image-guided procedure) and is most often guided by ultrasound [1]. One of the main challenges of this method is the inter-operative detection of the insertion needles and their corresponding seeds in the prostate. Due to the changes in the shape and volume of the prostate during the procedure, needles do not ideally follow the pre-treatment plan [2, 12], nor do the seeds remain in the same position once placed. Hence, localization of seeds (Figure 1) is necessary to: i) guide the surgeon during the treatment, and ii) modify the pre-treatment dosimetry plan accordingly to avoid under- or over-radiation dosage of the prostate and surrounding tissue [3].

Computed tomography (CT), magnetic resonance imaging (MRI), or trans-rectal ultrasound (TRUS) imaging can all be used to guide the Brachytherapy procedure. However, they all have their corresponding limitations. CT cannot be used to effectively detect the prostate boundary, and is not readily available during the operation [4, 5]. MRI is bulky, expensive and hard for surgeons to drive during the procedure. Ultrasound imaging possesses low signal to noise ratio resulting in "sub-optimal image quality when compared with the former techniques. However, it is significantly cheaper, mobile, and easy to operate during the surgery. Furthermore, it helps the physician to plan the location of the seeds in real time [6] rendering it the preferred way of imaging in Brachytherapy treatments.

In this paper, we propose an algorithm that calculates the needle paths and localizes their corresponding seeds using a set of transverse TRUS images. To this effect, a Gibbs Random Fields (GRF) [7] based approach is used to locate a given needle and its neighboring positions resulting in the calculation of a priori probabilities of the seeds belonging to the needle according to the dosimetry plan. Furthermore, we use 2D (in the X-Y plane) and 1D (along the Z-axis) Gaussian filters [8] to calculate the probability of the position of the needle and estimate the local maxima along its corresponding path. A cubic polynomial fit technique is employed to improve the calculated needle path. By using our proposed method, we effectively suppress the noise that affects the seed localization yielding a more accurate assignment of the seeds to their corresponding needle positions.

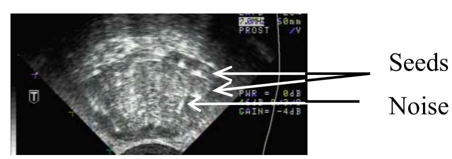

Figure 1: TRUS Image taken during the Brachytherapy procedure. Bright spots are either noise or seeds.

This paper is organized as follows. The proposed algorithm is discussed in Section 2. Results are provided in Section 3 and conclusions are drawn in Section 4.

2. PROPOSED ALGORITHM

Figure 2 shows a block diagram of our proposed approach. Here, we employ slices of TRUS images taken at 0.5 mm intervals during the Brachytherapy procedure (see Fig. 3). A pre-plan of the position of needles and the number of seeds inserted by each needle is assumed available a priori. The ground truth is established by utilizing CT to locate the seeds once the operation is complete. The needles are named and positioned according to the template shown in Figure 4.

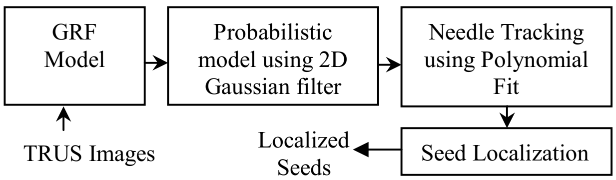

Figure 2: Block diagram of the algorithm for Seed Localization

A GRF based approach is used to model the likelihood of a given needle and its neighbors. Given the above along with the intensity profile of the region, the position of a given needle and its corresponding seeds are thereby estimated.

2.1. Brief Description of Brachytherapy

Brachytherapy is an advanced cancer treatment procedure. Radioactive seeds are placed in or near a given tumor, typically yielding an appropriate radiation dose to the tumor while reducing the radiation exposure to the surrounding healthy tissues [4]. These seeds are made of either Iodine-125 or Palladium-103 and are injected into the prostate using hollow needles. Possible locations where the needles can be inserted are limited by the template shown in Fig. 4. Typically 20-30 needles are placed, using the template, at various locations during the operation; and 40-120 seeds are inserted into the prostate dependent on its volume [1, 9]. The distance between each grid point in the template is 5mm along the horizontal and vertical directions [1]. A schematic of the apparatus is shown in Figure 3. The X and Y axes determine the transverse plane, and Y and Z axes determine the sagittal plane. TRUS images are then captured along the Z axis (transverse mode images) from apex to base of the prostate as shown in Figure 3.

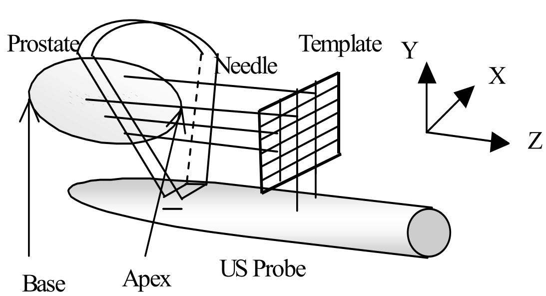

Figure 3: The schematic of the Brachytherapy Procedure with Transverse TRUS

2.2. GRF and Gaussian filters

We utilize a GRF based approach to model a given needle and its corresponding neighbors. In our model, the needle point and its neighboring 4 needle points are considered as shown in Figure 4 (see C1). A set of 2 point cliques are formed from these points and utilized to impose spatial

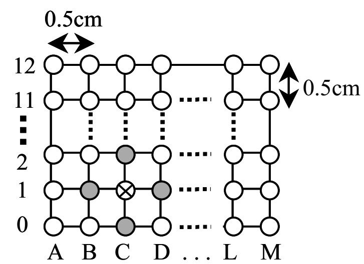

Figure 4: Scheme of the needle template. Any needle position (marked “x) and its 4 neighbors (grayed) form 2 point clique.

constraints during the search and localization procedure.

Let x denote a realization of a Gibbs Random Field X [7], and (i,j) define the location of interest in a second order neighborhood n_{ij}. The probability density function (pdf) of x is defined as a Gibbs Distribution:

$$p(x) = \frac{1}{z} e^{-E(x)} \tag{1}$$

where z is the normalizing constant and $E(x)$ is the energy function defined by:

$$E(x) = \sum_{c \in C} V_c(x) \tag{2}$$

where C denotes the set of all cliques. The energy function V for a pair-wise interaction model is defined as:

$$V_c(x) = \sum_{i,j=1}^{MN} G_{i,j} + \sum_{i,j=1}^{MN} \sum_{k,l=-1}^{1} H_{i,j;k,l} \qquad k \neq l \tag{3}$$

where M, N are the dimensions of the image, G is the potential function for single-pixel cliques, and H is the potential function for pair-wise cliques. According to [7], G and H are defined as:

$$G_{i,j} = \frac{w_{ij}}{\sqrt{2\pi}} e^{-\frac{1}{2}\left(\frac{\mu_{w0}^{ij} - 1}{\sigma}\right)^2} \tag{4}$$

$$H_{i,j;k,l} = \frac{w_r}{\sqrt{2\pi}} e^{-\frac{1}{2}\left(\frac{\mu_{wr}^{ij} - I(x_{i,j}, x_{k,l})}{\sigma}\right)^2} \tag{5}$$

where, $I(x_{i,j}, x_{k,l})=1$ if $x_{i,j} = x_{k,l}$ and 0 otherwise. w_{ij} and w_r are the weights associated with location (i,j) and with its neighboring points at distance r, respectively. The estimated mean values of the clique shapes at (i,j) of the random field are given by μ_{w0} and μ_{wr}, respectively. Once the likelihood model is created, Gaussian filters, along the transverse (X-

Y) plane and Z axis, are used to calculate the probability of the needle position of interest. These are defined as:

$$f(x,y) = \frac{1}{\sqrt{2\pi\sigma^2}} e^{-\frac{1}{2}\left(\frac{x^2+y^2}{\sigma^2}\right)} \qquad (6)$$

$$f(z) = \frac{1}{\sqrt{2\pi\sigma_z^2}} e^{-\frac{1}{2}\left(\frac{z^2}{\sigma_z^2}\right)} \qquad (7)$$

where *f(x,y)* is a 2D filter, *f(z)* is a 1D filter, σ is the variance along the X and Y axes and σ_z is the variance along the Z axis. The variance of the Gaussian filters is varied as a function of the full width - half maximum of the peak of the (2D or 1D) intensity profile.

2.3. Proposed Algorithm

For each given needle position in the pre-plan, perform algorithm steps 1through 6:

1) Calculate the GRF and the potential for each clique at the template coordinate system.
2) Apply the 2D Gaussian filter (Eq. 6) on this GRF and calculate the local maximum around the area of interest (around pre-planned needle position). Rescale to match the image size.
3) Find the local maximum of the TRUS acquired image, over the 41x41 window centered at the computed needle location found in Step 2. The position of the calculated TRUS peak is considered to be the new needle position and provides an initialization for the search at the next frame.
4) Repeat steps 1-3 through all slices in the scanned volume yielding an estimated needle path.
5) Due to the tissue non-homogeneity, edema, the shape of the needle tip (bevel versus diamond tip), and the insertion technique (rotation or pushing), the path of the needle diverges as we moves from the apex to the base of the prostate [2]. Hence a cubic polynomial fit is applied to update the position of the needle at the base. This is paired with the a priori needle position specified in the pre-plan. Once the needle path is estimated, the intensity profile along the path is calculated where each point is the sum of intensities of 25x25 window centered around the needle coordinates.
6) The intensity profile function is then smoothed using the 1D Gaussian filter (Eq. 7), and the seeds are located by finding the local primary maxima.

In the case of multiple seed insertions, multiple corresponding peaks separated by dips are found in the intensity profile. If these peaks are close to each other, they are assumed to be generated by a single seed. This may occasionally lead to the aggregation of two or more seeds. If the peaks are more than 10 slices apart (more that 5mm), they are assumed to represent two distinct seeds.

3. RESULTS

Our proposed algorithm was tested on sets of TRUS images obtained from 6 patients. Each patient's data consists of more than 120 TRUS images taken at 0.5 mm apart in the transverse imaging mode (see Fig. 3). The seed positions found using our algorithm are compared to the ground truth obtained from CT scans collected shortly after the operation [10]. A pre-plan indicating the template locations for needle insertion is also available at the beginning of the procedure.

Figure 5 shows the intensity profile along the path of the K7 needle as a function of the slice index for a given patient. According to the ground truth, two seeds were inserted by the K7 needle. The vertical lines mark the peaks found by our proposed algorithm from the filtered sub-images. Similarly, the algorithm is capable of effectively finding the remaining seeds.

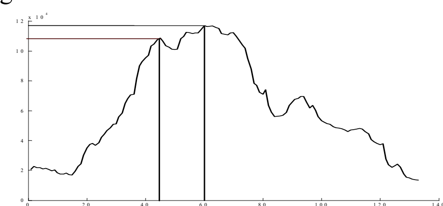

Figure 5: Intensity profile along the path of K7 needle

Figure 6 shows the needle-seed position pairing for a given patient TRUS images. From the figure, we can see that our proposed algorithm provides an accurate estimation of the needle and seed location when compared with the ground truth obtained from CT scans. The located seeds were within ±5 pixels in the *x, y* directions and ±10 slices in the *z* direction.

Subplot (a) of Figure 7 shows the C4 needle path across all the slices from the apex to the base of the prostate. From this plot, we can clearly see minimaldeflection in the path of the needle. Subplots (b) and (c) show the variation of the x and y positions respectively of the needle point along the entire volume. Subplot (d) shows the path of the needle in 2D sagittal view. Figure 8 illustrates the same details for the K5 needle using a different scale. In this figure, the dashed line shows the approximation of the needle path obtained by the polynomial fit. Note the significant increase in deflection (from approximately 0 to 0.5 cm deflection) in Figure 8 compared to the results shown in Figure 7 justifying our effective use of the polynomial fit in accounting for physical properties of the needle and inaccuracies in tracking. Table 1 demonstrates the improved seed localization obtained as a result of polynomial fitting.

Finally, the seed localization procedure was applied to the TRUS frames obtained from all 6 patients. The results indicate that our proposed approach was capable of detecting seeds and corresponding needle locations with an average accuracy of 86% and a range of 85% to 88%. This result represents an improvement over reported prior art [11].

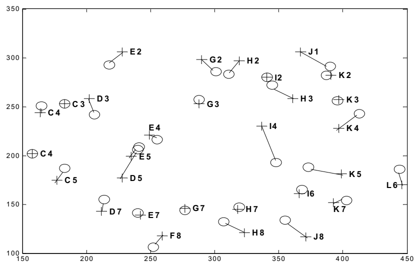

Figure 6. Needle positions pairing

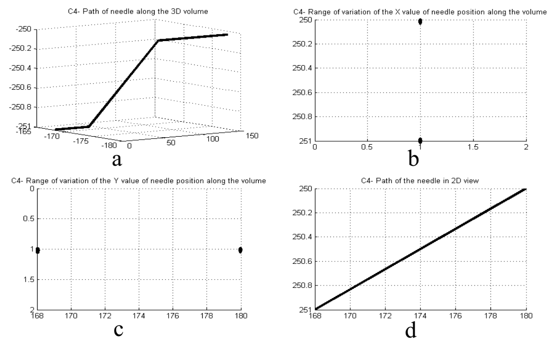

Figure 7. Needle Tracking for Needle C4

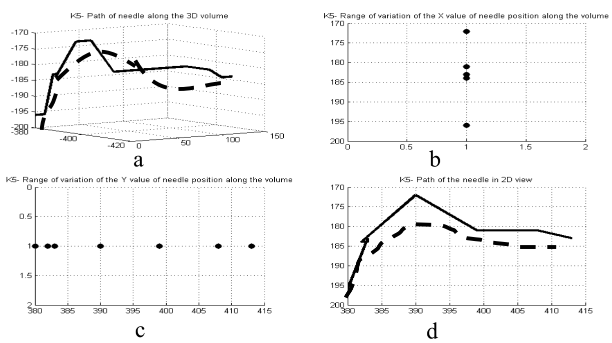

Figure 8. Needle Tracking for Needle K5

Table 1. Comparison of the number of seeds detected.

Patient	1	2	3	4	5	6
# of Seeds in plan	90	74	59	74	90	89
#Detected using pre-plan	50	46	33	42	48	54
#Detected using Simple Needle Tracking	73	68	50	64	74	79
#Detected using polyfit	79	68	55	66	80	82

4. CONCLUSIONS

In this paper, an algorithm for needle tracking and detection of seeds using a GRF framework was discussed. The GRF model and the application of Gaussian filters provide an effective methodology for estimating the position of the needle and its corresponding seeds with better accuracy than prior art. It was also observed that the polynomial fit allowed for a better approximation for the needle position and hence an improved detection of the corresponding implanted seeds. Future work will concentrate on the investigation of secondary maxima as potential seed locations, as well as on the use of the seed-needle pairing as a parameter for secondary decision criterion.

5. ACKNOWLEDGMENTS

This work was supported by the Electrical Engineering Department at RIT and partially supported by NIH/NCI grant R21 CA102236 and by grant R01 CA091763.

REFERENCES

[1] M.D. Rifkin, *Ultrasound of the prostate*, Raven Press, New York, 1988.

[2] T.K. Podder, L. Liao, J. Sherman, V. Misic, Y.D. Zhang, D. Fuller, D.J. Rubens, E.M. Messing, J.G. Strang, W.S. Ng, and Y. Yu, “Assessment of Prostate Brachytherapy and Breast Biopsy Needle Insertions and Methods to Improve Targeting Accuracy, *International Conference on Biomedical Engineering,* Singapore 2005.

[3] G. Cheng, H. Liu, L. Liao, Y. Yu, "Dynamic Brachytherapy of the Prostate Under Active Image Guidance", *Medical Image Computing and Computer-Assisted Intervention*, Utrecht, The Netherlands, 2001

[4] E.J. Holupka, P.M. Meskell, E.C. Burdette, I.D. Kaplan, “An automatic seed finder for Brachytherapy CT post-plans based on the Hough transform, *Med. Phys. 31*, 2672 ,2004.

[5] S.T. Lam, P.S. Cho, R.J. Marks II, S. Narayanan, “Detection and correction of patient movement in prostate Brachytherapy seed reconstruction, *Phys. Med. Biol.* 50, 2071-2087, 2005.

[6] S.T. Lam, P.S. Cho, R.J. Marks II, S. Narayanan, “Three-dimensional seed reconstruction for prostate Brachytherapy using Hough trajectories, *Phys. Med. Biol.* 49, 557-569, 2004.

[7] R.M. Mohamed, A. El-Baz, A.A. Farag, “Image Modeling Using Gibbs-Markov Random Field and Support Vector Machines Algorithm*,” International Journal of Information Technology*, vol 1 number 4, 2004.

[8] R.C. Gonzalez, R.E. Woods, *Digital Image Processing*, s.e. Prentice Hall Inc., New Jersey, 2001.

[9] D.A. Todor, M. Zaider, G.N. Cohen, M.F. Worman, M.J. Zelefsky, “Intra-operative dynamic dosimetry for prostate implants, *Phys. Med. Biol.* 48, 1153-1171, 2003.

[10] H. Liu, G. Cheng, Y. Yu, et al., "Automatic localization of implanted seeds from post-implant CT images", *Phys. Med. Biol.* 48 1191-1203, 2003.

[11] B.H. Han, K. Wallner, G. Merrick, W. Gregory, S. Sutlief, “Prostate Brachytherapy seed identification on post-implant TRUS images , *Med. Phys, 30 (5)* pp.898-90, 2003.

[12] G. Wan , Z. Wei , L. Gardi , D.B. Downey, A. Fenster , “Brachytherapy needle deflection evaluation and correction, *Med Phys. 32*(4),902-9, Apr 2005.